Octahydroacridine thin films grown by matrix-assisted pulsed laser evaporation for non linear optical applications

Valentin Ion[a], Andreea Matei[a], Catalin Constantinescu[a,*], Iulian Ionita[a,b], Maria Marinescu[c], Maria Dinescu[a], Ana Emandi[c,d]

[a]INFLPR—National Institute for Laser, Plasma and Radiation Physics, 409 Atomistilor Blvd., Magurele, Bucharest RO-077125, Romania
[b]UB—University of Bucharest, Faculty of Physics, 405 Atomistilor Blvd., Magurele, Bucharest RO-077125, Romania
[c]UB—University of Bucharest, Faculty of Chemistry, Department of Inorganic Chemistry, 90-92 Panduri St., Bucharest RO-050663, Romania
[d]INOE 2000—National Institute for Optoelectronics, 409 Atomistilor Blvd., Magurele, Bucharest RO-077125, Romania

We report on the thin film growth of *1,2,3,4,5,6,7,8-octahydroacridine* (OHA) by matrix-assisted pulsed laser evaporation (MAPLE), starting from a frozen solution of 1% OHA dissolved in methanol and using a Nd:YAG laser emitting at 266 nm wavelength with fluences in the range 0.1–1 J/cm^2. The optical properties were studied by spectroscopic-ellipsometry (SE), while Fourier transform infrared spectroscopy (FTIR), atomic force microscopy (AFM), and scanning electron microscopy (SEM) were performed for structure and surface morphology investigation. Second harmonic generation (SHG) capabilities of the thin films were investigated by using a tunable Ti:sapphire laser with maximum emission centred in near infra-red. The peak of emitted photons is located at 388 nm, therefore half the wavelength of the initial photons (776 nm). The semi logarithmic dependence of SHG intensity on incident power is almost linear, except the value obtained at highest power of incident photons. This value indicates a local changing of sample due to the heating produced by the high-power incident beam.

1. Introduction

Acridine ($C_{13}H_9N$) is a stable, weakly basic compound, structurally related to anthracene ($C_{14}H_{10}$) with one of the central CH groups replaced by nitrogen [1,2]. Pure acridine was first isolated in 1871 by Carl Gräbe and Heinrich Caro, as it naturally occurs in coal tar. Its derivatives are a class of materials with a large area of applications, most of them known human carcinogens, causing frameshift mutations by incorporating into the DNA and creating an additional base on the opposite strand [1–5]. They have been widely used as antibacterial and antiprotozoal agents, *e.g.* the acridone derivatives, synthesized by the *Lehmstedt-Tanasescu* reaction [6,7], or other type of drugs [1,3–5]. In the last few years, the acridine-based compounds drew attention upon their non-linear optical properties [8–10]. One such compound is *1,2,3,4,5,6,7,8-octahydroacridine* ($C_{13}H_{17}N$) or OHA, a white crystalline solid that is less toxic compared to acridine [11,12]. OHA and its derivatives are of great interest as they play an important role in the preparation of agrichemicals, alkaloids, dyes, medicines, drugs and other biologically active compounds with intriguing pharmacological and therapeutic properties in cancer and Alzheimer's disease treatments, and advanced functional materials precursors [1,2,13,14]. Today, OHA can be easily synthesized by different routes [14–30], making it an economically attractive candidate for various

* Corresponding author.
E-mail address: catalin.constantinescu@inflpr.ro (C. Constantinescu).

applications due to its excellent price/quality ratio. Among these applications, non-linear optical (NLO) properties that may arise from particularities of the OHA molecule (*i.e.* influence of conformational asymmetry due to the tricyclic structure) make it suitable for bulk and thin film second harmonic generation (SHG) investigations [30,31].

Here, we report on the deposition of OHA thin films by matrix-assisted pulsed laser evaporation (MAPLE), starting from a frozen solution of 1% OHA dissolved in methanol. The optical properties of the films were studied by spectroscopic-ellipsometry (SE). Fourier transform infrared spectroscopy (FTIR), atomic force microscopy (AFM), and scanning electron microscopy (SEM) were employed for structure and surface morphology investigation. SHG capabilities of OHA thin films were evidenced by using a femtosecond pulsed laser.

2. Experimental

Direct laser irradiation, *e.g.* by pulsed laser deposition (PLD) of organic molecules may induce photo-chemical decomposition and pyrolysis [32]. The MAPLE technique uses an absorbing matrix (i.e. the solvent, typically using concentrations of 1–4%) that acts like a protection for the molecules [32–34], although some interesting inverse effects have recently also been pointed out [35]. Furthermore, the MAPLE technique is also suitable in making multilayered thin films and/or embedded structures, when no compatible solvents are available for simpler techniques, such as spin coating, dropcasting, and dip-coating.

In our MAPLE experiments we used a 1% solution of laboratory synthesized OHA [24,30], carefully frozen in liquid nitrogen in a copper target holder [36–39]. The target holder was kept solid throughout thin film growth procedures. From our previous experience and based on literature studies [34–40], the laser fluence was chosen in the range of 0.1–1 J/cm^2 (Nd:YAG, "Surelite II" pulsed laser system from Continuum Company: 266 nm wavelength, 7 ns duration of the pulse, 10 Hz), using a 2 mm² spot. All depositions took place in vacuum (1×10^{-4} mbar), with the chamber being continuously pumped by a "Pfeiffer-Balzers 4 TPU 170" turbomolecular system (170 l s^{-1} volume flow rate). The target was irradiated with 40000 laser pulses, in order to evidence thin film thickness dependence to its morphology and optical properties. The substrates, i.e. polished Si wafer (on both sides), and indium tin oxide (ITO) covered BK7 glass slides, were kept at room temperature during thin film growth. Prior to the deposition, the substrates were cleaned by ultrasonic bath for 15 min, using acetone and isopropanol as cleaning mediums, and then dried in nitrogen gas flow. The target—substrate distance was chosen to be 3.5 cm, with the target rotated during MAPLE.

Thin film morphology and surface roughness were analyzed by atomic force microscopy (AFM) using a "XE-100" setup produced by Park Systems. These investigations were made in non-contact mode using a silicon carbide tip (10 nm radius of curvature). Fourier transform infrared absorption spectra of the OHA thin films grown by MAPLE on double side polished Si wafers were compared to the dropcast films. The measurements have been performed using a Jasco 6300 FTIR machine, in the range 400–4000 cm^{-1} (resolution: 4 cm^{-1}). Optical measurements were performed by using a Woolam Vertical Variable Angle Spectroscopic Ellipsometer (V-VASE), equipped with a high-pressure Xe discharge lamp incorporated in an HS-190 monochromator. Spectroscopic-ellipsometry measurements were performed between 400 and 1000 nm spectral range (step of 2 nm), and fixed angle of incidence (60°). The investigations of SHG capabilities were made using a setup that includes: a tunable Ti:sapphire laser with maximum emission centred at 800 nm (Spectra Physics, 60–100 fs pulse duration, 80 MHz repetition rate, 700 mW output power); an optical system that allows the variation of beam intensity (made using a half-wave plate and a *Glan–Taylor* polarizing prism, that allows to reach continuous range of 0–400 mW); and a microscope objective ($20 \times$) that focalizes the laser beam onto the OHA thin film samples. The intensity of the emitted SHG radiation is collected through fiber-optic cables and measured by an iCCD camera spectrograph from ANDOR.

3. Results and discussion

3.1. Fourier transform infrared spectroscopy

FTIR absorption measurements have been performed on the starting material, as a dropcast thin film, in order to get the corresponding OHA fingerprint. The results were compared to those originating from thin films deposited by MAPLE, in order to identify the best deposition conditions.

In Fig. 1, two spectra are presented, corresponding to the starting material (dropcasted), and to the MAPLE grown thin film, grown at 0.3 J/cm^2. One can immediately notice the resemblance between the OHA dropcasted film vs. the MAPLE one, pointing out its structural preservation upon laser processing. The OHA-related vibrations can be grouped as follows: vibrations originating from the pyridine ring and vibrations due to aliphatic cycle, respectively [13,14]. The spectrum consists in the acridine characteristic vibrations, combined with the vibrations of the simple bonds from the aliphatic group [41,42]. Specifically, the peaks observed at approximately 1520 cm^{-1} and 1599 cm^{-1} are related to the ring stretching vibration of the pyridine compound. The bands positioned at 2911 cm^{-1} and 2839 cm^{-1} are related to the

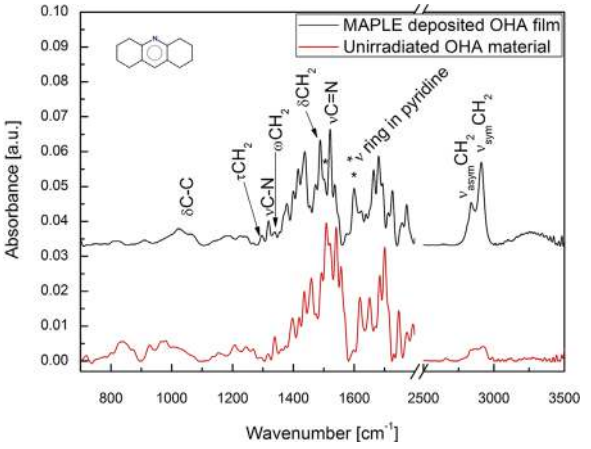

Fig. 1. FTIR absorption spectra of dropcast vs. MAPLE grown OHA thin films (0.3 J/cm^2 laser fluence, 2 mm^2 laser spot area, 40 000 pulses), and the molecular structure of OHA (upper left side inserted image).

asymmetric and symmetric –CH_2– stretching vibrations while the peaks at 1487 cm^{-1} and 1296 cm^{-1} correspond to the deformation and twisting –CH_2– vibrations. The peak at 1377 cm^{-1} is attributed to –CH2– wagging vibrations. The C–C skeletal deformation vibration can be identified at 1025 cm^{-1}. Finally, the C=N and C–N stretching vibrations can be identified at 1540 cm^{-1} and 1318 cm^{-1}, respectively.

3.2. Atomic force microscopy

The AFM analysis of the thin films surface revealed smooth surface, with just a few droplets covering the structure. Different surface sizes, and areas, were scanned on the samples; 40×40 μm^2 and 10×10 μm^2 AFM images are presented in Fig. 2. AFM investigations are needed in order to evaluate the uniformity of the surface before further optical, SE, and SHG investigations.

The MAPLE-grown thin films exhibit roughness typically around 5 nm, expressed as root mean square (RMS), at a thickness of 60 nm (determined by SE measurements, as described in Section 3.3). The roughness evaluation was made over a series of three samples, on large area scans (40×40 μm^2) with different scanned zones for each sample [43]. The morphology of the films is directly linked to the laser–frozen target interaction: droplets and other types of fragments may be ejected from the frozen target during MAPLE and collected on the thin film, and/or degradation of the OHA molecular structure by releasing gas and particulates that influence the thin film growth mechanism due to the laser induced thermal effects [33–37,44–46]. Since the films are of low roughness, this makes them suitable for further optical and SHG investigations.

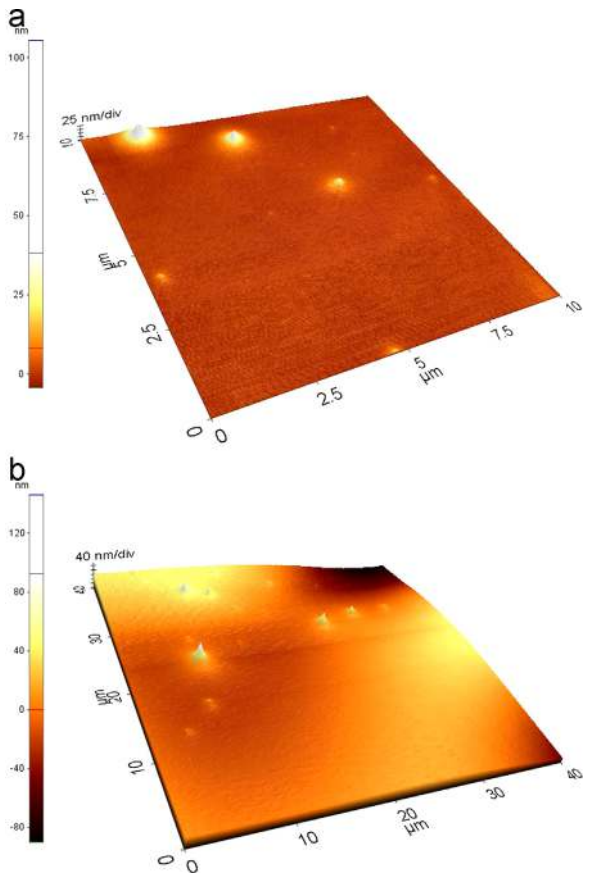

Fig. 2. AFM images on MAPLE grown OHA thin films (0.3 J/cm^2 laser fluence, 2 mm^2 laser spot, 31 000 pulses), on ITO-covered glass substrates: 10×10 μm^2 (a) and 40×40 μm^2 (b).

3.3. Optical and spectroscopic-ellipsometry investigations

The OHA thin film samples grown on silicon substrates were measured by using the Cauchy–Urbach formalism: approximated with a material with Cauchy dispersion with Urbach absorption [47]. The optical model used for fitting the experimental data consisted, in a first approach, of 4 layers: a Si bulk substrate, a native SiO_2 layer with thickness 3 nm, OHA and a rough top layer. The rough layer is composed of OHA and air in 50:50 ratio, using the Bruggeman effective medium (B-EMA) approximation [47]. The values for the bulk dielectric functions of Si and SiO_2 substrates were taken from literature [48].

In Fig. 3, the experimental parameters (ψ and Δ) and modeled curves are presented. The value of the mean squared error (MSE) is 11.93, and the Cauchy–Urbach parameters are $A_n = 1.551$; $B_n = 0.012$; $A_k = 0.194$, $B_k = 0.448$. Thin film thickness was found to be 41.51 nm with 24.15 nm roughness. Because of high value of roughness of thin film, the optical model was reconsidered. In a second step, the OHA thin film was considered to be inhomogeneous. For this purpose, it was chosen a specific wavelength from the measured spectrum ($\lambda = 500$ nm) and considered to be thickness graded. In this case, we determined that the refractive index and extinction coefficient are variable with thickness. The Cauchy–Urbach parameters were found to be: $A_n = 1.452$; $B_n = 0.013$; $A_k = 0.175$, $B_k = 0.523$. MSE value is 8.728, at 60.73 nm thickness, and with a 5.31 nm roughness. The value of roughness is in good agreement with the AFM results. By using the above parameters to generate the medium of refraction and extinction coefficients, we obtain $n \sim 1.49$ and $k = 10^{-2}$ in the visible region of the spectrum (600 nm), as presented in Fig. 4a and b. The transmission of the OHA thin films, grown on ITO covered BK7 glass substrates, was also investigated

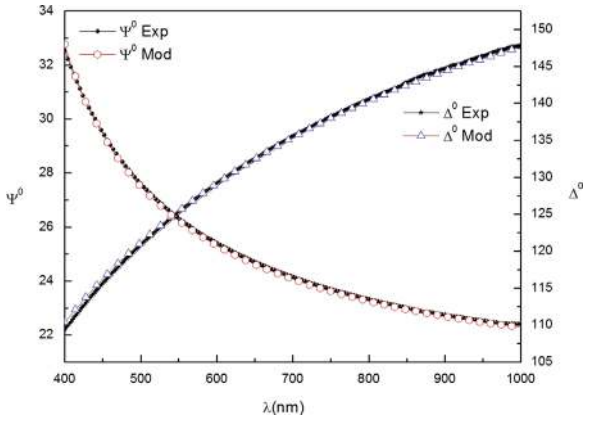

Fig. 3. The experimental and modeled spectra (ψ and Δ) of MAPLE grown OHA thin films (0.3 J/cm^2 laser fluence, 2 mm^2 laser spot, 40 000 pulses), on Si substrates.

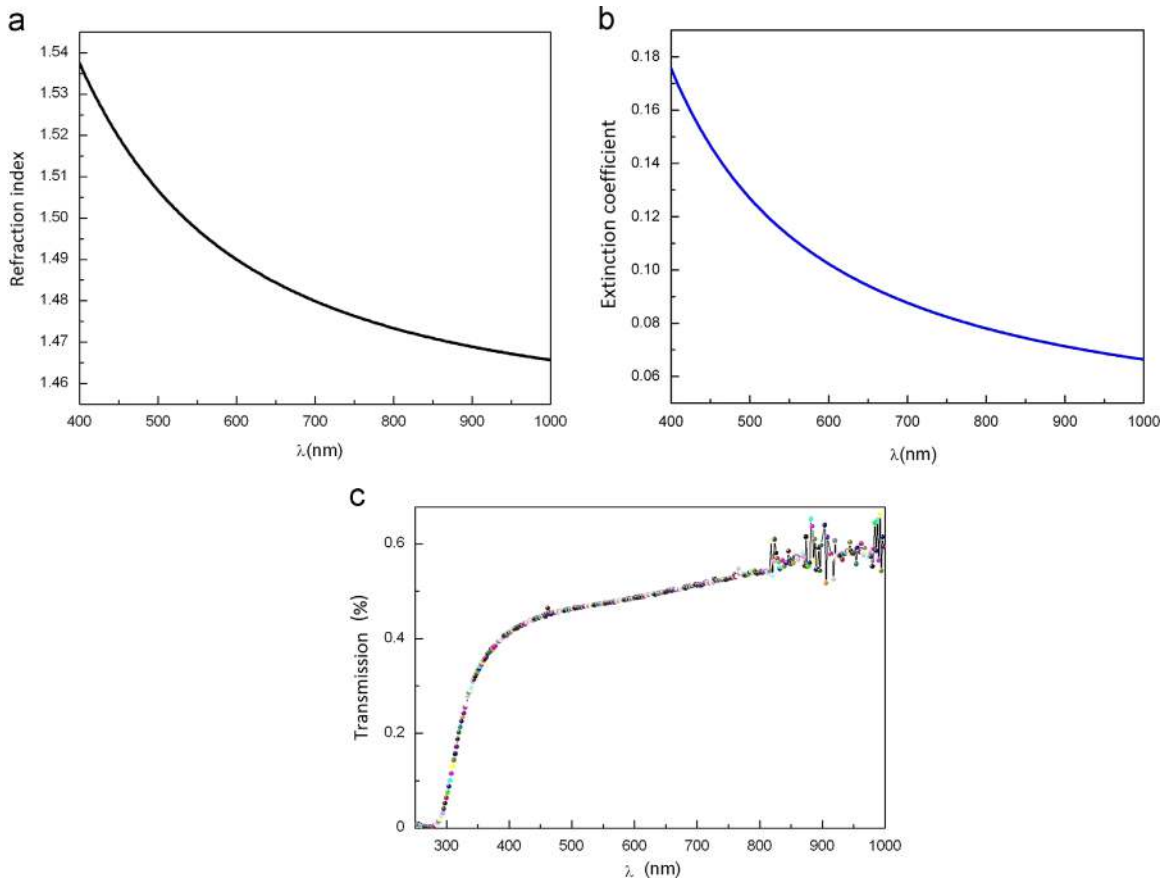

Fig. 4. The refraction index (a), extinction coefficient (b), and the transmission spectra for OHA thin films, grown on ITO-covered BK7 substrates (c) (thin film growth conditions: 0.3 J/cm^2 laser fluence, 2 mm^2 laser spot, 40 000 pulses).

between 250 and 1000 nm wavelength (UV–vis spectroscopy). One can observe that the films are about 50% absorbent in the range 450–800 nm (Fig. 4c). The refractive index depends on the thickness of the sample, as presented in Fig. 5. The highest value of n was obtained at the substrate interface and it decreases slowly for thicker films. This behaviour can be explained by the density inhomogeneity of the thin film: the film seems to have a higher density at the substrate interface, most probably due to solvent effects from the MAPLE deposition technique used here [34]. The extinction coefficient was found to be 10^{-1}–10^{-2}; the optical absorption is related to the film defects (voids).

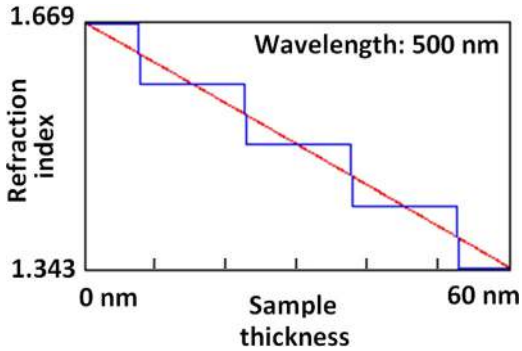

Fig. 5. The refraction index dependence vs. thickness of the OHA samples, at a chosen wavelength (λ=500 nm).

3.4. Second harmonic generation

Since mediums with inversion symmetry are forbidden from generating second harmonic light, surfaces and interfaces make interesting subjects for study with SHG. In fact, second harmonic generation and sum frequency generation discriminate against signals from the bulk, implicitly labelling them as surface specific techniques.

The SHG spectra of OHA thin films under irradiation at 776 nm are presented in Fig. 6a. The peak of emitted photons is located at 388 nm, therefore half the wavelength of the initial photons. Also, the half maximum bandwidth (HMBW) of SHG emission band of about 8 nm is in a good agreement with the HMBW of incident laser light of 100 fs pulsed length. The intensity of the emitted radiation with respect to the power of the incident beam is presented in Fig. 6b. The semi logarithmic dependence of SHG intensity on incident power is almost linear, except for the values obtained at the highest power of the incident photons. This value indicates a local changing of the sample due to the heating produced by the high power beam. The slope value of linear fitting is 3868 intensity units/W^2. This single value has not any signification, due to the fact that the entire detection system was not

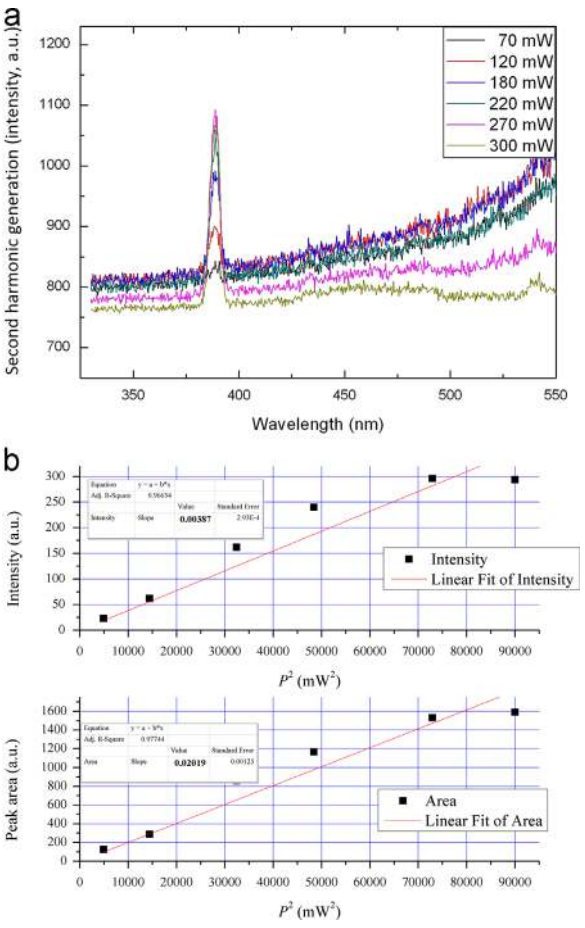

Fig. 6. The SHG experimental spectra of MAPLE grown OHA thin films (0.3 J/cm^2 laser fluence, 2 mm^2 laser spot, 40 000 pulses), on Si substrates, under fs-laser irradiation at 788 nm wavelength (a). In (b), the efficiency slope for the SH intensity vs. laser power: the slope value of linear fitting is 3868 intensity units/W^2.

calibrated in power units as the incident beam was. However, the line slope is proportional to the SH coefficient and is a good indication of the sample's SHG behaviour. It is useful to compare different samples, measured in the same conditions, in order to select the most appropriate for the desired application. The presence of the SHG signal is related to the conformational asymmetry of the OHA molecule [14]. Nevertheless, this makes OHA films to be of low-to-medium capability for SHG applications.

As a final aspect of our work, we have to take into consideration that the chemical structure, the crystalline state, and thus the homogeneity of the sample, all play a very important part in its SHG capabilities [49]. It is also worth mentioning that, for the thin films, the thickness, but also the surface morphology, plays an important role in the SHG intensity [50–55].

3.5. Octahydroacridine thin films for non-linear optics and potential applications

Up to this date, no consistent experimental results and/or numerical investigations, regarding OHA for applications in nonlinear optics, have been reported in literature. There is also a gap when searching for studies that are discussing on applications using such thin films. Common non-linear optical applications include optical limiting, spectroscopic and electrochemical sensing, second harmonic generation, etc. Surface SHG is very useful for monitoring the growth of monolayers on a surface: as particles adsorb, the SHG signal is altered. For example, common applications in surface science are related to the adsorption of small gas molecules. By using OHA thin films in sensor devices, one can probe the amount of a certain type of gas molecules attached to the sensor surface, after specific calibration. As the first monolayer forms, the intensity will increase to a maximum until a uniform distribution of particles is obtained. Further on, as additional particles adsorb and the second monolayer begins to form, the SHG signal will decrease until it reaches a minimum at the completion of the second monolayer [49]. As additional layers form, the SHG response of the substrate is screened by the adsorbate and eventually, the SHG signal will level off. In surface spectroscopy, details can be determined about the electronic structure and band gaps, since either the fundamental or second harmonic are resonant with electronic transitions in the surface atoms. Finally, molecular orientation can be probed by observing the polarization of the second harmonic signal, generated from a polarized beam, and this can also be used to monitor chemical reactions at a surface with picosecond resolution.

4. Conclusion

We present results on thin film growth by MAPLE technique of *1,2,3,4,5,6,7,8-octahydroacridine*. Typically, the films exhibit roughness of ~5 nm, as determined by atomic force microscopy and spectroscopic-ellipsometry. The thin films reproduce the chemical structure of the starting material, particularly when grown at low fluences (0.3 J/cm^2) as revealed by the Fourier transform infrared spectroscopy measurements. Finally, we discuss on the second harmonic generation capabilities of the films and show that the peak of emitted photons is located at 388 nm, therefore half the wavelength of the initial photons (776 nm) and emphasize that the signal is related to the conformational asymmetry of the molecule, but also to surface and interface effects. The results that we present here, for smooth/compact *1,2,3,4,5,6,7,8-octahydroacridine* thin films grown by matrix-assisted pulsed laser evaporation, open the path for further investigations in order to maximize the second harmonic signal, and to further use in optoelectronic devices particularly in spectroscopic and/or specific electrochemical sensing.

Acknowledgements

We gratefully acknowledge the help, suggestions and comments, provided by *Dr. Bogdana Mitu* for the FTIR measurements, and *Dr. Mihaela Filipescu* for the AFM investigations. This work was supported by a grant of the Romanian National Authority for Scientific Research, CNCS—UEFISCDI, project number **PN-II-PT-PCCA-2011-3.2-0394** (contract **PCCA 17/2012**)—"*NANOCEA*".

References

[1] A. Adrien, The Acridines: Their Preparation, Physical, Chemical, and Biological Properties and Uses, Eward Arnold & Co, London, 1951.
[2] R.M. Acheson, Chemistry of Heterocyclic Compounds: Acridines, second ed. John Wiley & Sons Inc., New York, 1973 ISBN: 0-471-37753-8.
[3] R.K. Herman, N.B. Dworkin, J. Bacteriol. 106 (1971) 543–550.
[4] G.P. Moloney, D.P. Kelly, P. Mack, Molecules 6 (2001) 230–243.
[5] L.S. Lerman, J. Mol. Biol. 3 (1961) 18–30.
[6] I. Tănăsescu, Bulletin de la Societe Chimique de France 41 (1927) 528.
[7] K. Lehmstedt, Berichte der deutschen chemischen Gesellschaft 65 (1932) 834–839.
[8] H. Singh Nalwa, Adv. Mater. 5 (1993) 341–358.
[9] A. Molinos-Gomez, X. Vidal, M. Maymo, D. Velasco, J. Martorell, F. Lopez-Calahorra, Tetrahedron 61 (2005) 9075–9081.
[10] D. Avci, H. Comert, Y. Atalay, J. Mol. Model. 14 (2008) 161–169.
[11] TCI America, Material Safety Data Sheet: 1,2,3,4,5,6,7,8-Octahydroacridine (2005) 1-3; available at ⟨https://www.spectrumchemical.com/MSDS/TCI-O0197.pdf⟩.
[12] S.H. Mikkelsen, S. Havelund, A.S. Mogensen, F. Stuer-Lauridsen, Survey of Chemical Substances in Consumer Products 59 (2005) 64–65.
[13] A. Canas-Rodriguez, R.G. Canas, A. Mateo-Bernardo, Chem. Abstr 108 (1988) 112191t.
[14] G.R. Newkome, The chemistry of heterocyclic compounds, Pyridine and Its Derivatives, 14, John Wiley & Sons Inc., New York, 2009 ISBN: 978-0-470-18820-0.
[15] V.A. Stonik, V.I. Vysotskii, M.N. Tilichenko, Chem. Heterocycl. Compd. 6 (1970) 1439–1443.
[16] M.R. Del Giudice, A. Borioni, C. Mustazza, F. Gatta, J. Heterocycl. Chem. 34 (1997) 1661–1667.
[17] M.L. Pilato, V.J. Catalano, T.W. Bell, J. Org. Chem. 66 (2001) 1525–1527.
[18] A.F. Borowski, S. Sabo-Etienne, B. Donnadieu, B. Chaudret, Organometallics 22 (2003) 1630–1637.
[19] R.G. Jacob, G. Perin, G.V. Botteselle, E.J. Lenardao, Tetrahedron Lett. 44 (2003) 6809–6812.
[20] S.J. Kulkarni, K.V.V. Krishna Mohan, V.R. Rani, N. Narender, K.V. Raghavan, Stud. Surf. Sci. Catal. 154 (2004) 2781–2787.
[21] D. Regas, M.M. Afonso, J.A. Palenzuela, Syn.-Stuttgart 5 (2004) 757–760.
[22] A. Ratnamala, V. Durga Kumari, M. Subrahmanyam, N. Archana, Chem. Commun. (2004) 2710–2711.
[23] J.S. Yadav, B.V.S. Reddy, L. Chetia, G. Srinivasulu, A.C. Kunwar, Tetrahedron Lett. 46 (2005) 1039–1044.
[24] F. Potmischil, M. Marinescu, T. Loloiu, Revista de Chimie 58 (2007) 795–798.
[25] F. Potmischil, M. Marinescu, A. Nicolescu, C. Deleanu, M. Hillebrand, Magn. Reson. Chem. 46 (2008) 1141–1147.
[26] A. Ratnamala, K. Lalitha, J.K. Reddy, V.D. Kumari, M. Subrahmanyam, J. Mol. Catal. A: Chem. 279 (2008) 112–118.
[27] Q.F. Wang, C.G. Yan, Cent. Eur. J. Chem. 6 (2008) 404–409.
[28] F. Potmischil, M. Marinescu, A. Nicolescu, C. Deleanu, Magn. Reson. Chem. 47 (2009) 1031–1035.
[29] J.E.R. Nascimento, A.M. Barcellos, M. Sachini, G. Perin, E.J. Lenardao, D. Alves, R.G. Jacob, F. Missau, Tetrahedron Lett. 52 (2011) 2571–2574.
[30] M. Marinescu, C. Tablet, F. Potmischil, M. Hillebrand, Spectrochim. Acta Part A 81 (2011) 560–569.
[31] T. Masamune, J. Am. Chem. Soc. 79 (1957) 4418–4423.
[32] T. Lippert, D.B. Chrisey, A. Purice, C. Constantinescu, M. Filipescu, N.D. Scarisoreanu, M. Dinescu, Romanian Rep. Phys. 59 (2007) 483–498.
[33] R. McGill, D. Chrisey; Method of Producing a Film Coating by Matrix-assisted Pulsed Laser Deposition, US Patent Number: 6025036, Issue Date: February 15th 2000.
[34] A. Luches, A. Piqué, L.V. Zhigilei (Issue Editors), in Appl. Phys. A: Mater. Sci. Process. 105 issue 3 (2011) 517-701.
[35] M. Tabetah, A. Matei, C. Constantinescu, N.P. Mortensen, M. Dinescu, J. Schou, L.V. Zhigilei, J. Phys. Chem. B 118 (2014) 13290–13299.
[36] C. Constantinescu, L. Rapp, P. Rotaru, P. Delaporte, A.P. Alloncle, Chem. Phys. 450–451 (2015) 32–38.
[37] E. Morintale, C. Constantinescu, M. Dinescu, Phys. AUC 20 (2010) 43–56.
[38] C. Constantinescu, A. Emandi, C. Vasiliu, C. Negrila, C. Logofatu, C. Cotarlan, M. Lazarescu, Appl. Surf. Sci. 255 (2009) 5480–5485.
[39] A. Matei, S. Canulescu, C. Constantinescu, J. Schou, M. Dinescu, AIP Conference Proceedings. 1464 (2012) 256–264.
[40] V. Dinca, P.E. Florian, L.E. Sima, L. Rusen, C. Constantinescu, R.W. Evans, M. Dinescu, A. Roseanu, Biomed. Microdevices 16 (2014) 11–21.
[41] G. Socrates, Infrared Characteristic Group Frequencies, second ed. J. Wiley & Sons Ltd, 1994.
[42] M. Avram, G.h.D. Mateescu, Infrared Spectroscopy—Application in Organic Chemistry, Wiley—Interscience, New York, 1972.
[43] V.N. Koinkar, B. Bhushan, J. Appl. Phys. 81 (1997) 2472–2479.
[44] E. Leveugle, L.V. Zhigilei, J. Appl. Phys. 102 (2007) 074914.
[45] C. Constantinescu, E. Morintale, V. Ion, A. Moldovan, C. Luculescu, M. Dinescu, P. Rotaru, Thin Solid Films 520 (2012) 3904–3909.
[46] C. Constantinescu, A. Rotaru, A. Nedelcea, M. Dinescu, Mater. Sci. Semicond. Process. 30 (2015) 242–249.
[47] Hiroyuki Fujiwara, Spectroscopic Ellipsometry Principles and Applications, Published by Maruzen Co. Ltd, Tokyo, Japan, 2007 ISBN-13: 978-0-470-01608-4.
[48] C. Herzinger, B. Johs, W. McGahan, W. Paulson, J. Woollam, J. Appl. Phys. 83 (1998) 3323–3336.
[49] R. Menzel, Photonics. Linear and Non-linear Interactions of Laser Light and Matter, Springer, Berlin Heidelberg, 2007 ISBN 978-3-540-45158-7.
[50] A. Stanculescu, L. Vacareanu, M. Grigoras, M. Socol, G. Socol, F. Stanculescu, N. Preda, E. Matei, I. Ionita, M. Girtan, I.N. Mihailescu, Appl. Surf. Sci. 257 (2011) 5298–5302.
[51] I.M. Craig, C.J. Tassone, S.H. Tolbert, B.J. Schwartz, J. Chem. Phys. 133 (2010) 044901.
[52] A. Matei, C. Constantinescu, B. Mitu, M. Filipescu, V. Ion, I. Ionita, S. Brajnicov, A.P. Alloncle, P. Delaporte, A. Emandi, M. Dinescu, Appl. Surf. Sci. (2015). in press, http://dx.doi.org/10.1016/j.apsusc.2014.11.022.
[53] C. Constantinescu, A. Matei, I. Ionita, V. Ion, V. Marascu, M. Dinescu, C. Vasiliu, A. Emandi, Appl. Surf. Sci. 302 (2014) 69–73.
[54] A. Matei, C. Constantinescu, V. Ion, B. Mitu, I. Ionita, M. Dinescu, C. Vasiliu, A. Emandi, J. Org. Chem. 751 (2014) 638–643.
[55] C. Constantinescu, A. Matei, V. Ion, B. Mitu, I. Ionita, M. Dinescu, C.R. Luculescu, C. Vasiliu, A. Emandi, Appl. Surf. Sci. 302 (2014) 83–86.